


Discrete heat equation for a periodic layered system with allowance for the interfacial thermal resistance: General formulation and dispersion analysis

S. L. Sobolev 

Federal Research Center of Problems of Chemical Physics and Medicinal Chemistry, Russian Academy of Sciences, Chernogolovka, Moscow Region 132432, Russia
and Samara State Technical University, ul. Molodogvardeiskaya 244, Samara 443100, Russia



(Received 21 January 2024; accepted 8 April 2024; published 1 May 2024)

Discrete heat equations for the multilayered periodic systems with allowance for the thermal resistance between the layers and corresponding dispersion relations in $\omega-k$ space have been derived and analyzed. The discrete equations imply a finite velocity of thermal disturbances and guarantee the positiveness of the solutions. Analytical expressions for the attenuation distance, and phase and group velocities have been obtained as functions of frequency and thermal resistance between the discrete layers. These functions demonstrate unusual behavior at high frequency compared to the continuum case. Furthermore, the maximum allowed frequency and wave number for the discrete heat equation are limited, whereas there are no such limits in a continuum. The discrete equation contains an infinite hierarchy of continuous partial differential equations, which starts with the Fourier law, proceeds with the hyperbolic equation, the Guyer-Krumhansl (or Jeffreys type) equation, and then with higher-order equations. The partial differential equations with a finite number of terms are only approximations of the discrete equation, which implies that on the ultrashort space and timescales the discrete approach is preferable. This work provides a relatively simple, easy-to-adopt, conceptual tool, together with analytical expressions allowing one to study ultrafast wavelike heat conduction regimes in periodic multilayered metamaterials.

DOI: [10.1103/PhysRevE.109.054102](https://doi.org/10.1103/PhysRevE.109.054102)

I. INTRODUCTION

In recent years, there is a growing community from different disciplines interested in the different aspects of transport processes occurring on ultrashort time and space scales such as heat conduction in layered correlated materials [1,2] and nanosized systems [3–7], second sound [8], nonlocal diffusion in nanosized systems [9–13] and during drug release [14,15], and heat conduction under femtosecond laser irradiation [16]. The interest is motivated not only by technological needs, but also by unusual non-Fourier and non-Fickian phenomena arising on ultrashort space and/or time scales [17,18]. For example, the classical Fourier description is not able to explain such phenomena as wavelike temperature propagation [1–3,8], size-dependent [19–21] and distance-dependent [19] thermal conductivity across nanofilms, boundary temperature jump at the interfaces [19–25], and thermoelectricity effects [26]. An extensive body of literature exists on the theoretical description of the non-Fourier and non-Fickian effects (see, e.g., Refs. [3–7,9–16] and recent reviews [17,18]). However, most of the non-Fourier approaches are based on the continuum hypothesis, which assumes that both time and space are continuous variables. In contrast to the conventional continuous description, the discrete variable model (DVM) assumes that the space and time are discrete variables [19,20,27–43]. The basic concept of the DVM is to develop a relatively

simple model that includes into consideration the essential physics of the transfer process, that is, the space and time nonlocality. The nonlocal effects play an important role on ultrashort space and time scales when the characteristic space and/or time scales begin to be comparable to the mean free path (MFP) and/or mean free time (MFT) of energy carriers. In addition, the discrete description is relevant for processes of many physical contexts, such as calcium burst waves in living cells, propagation of action potentials through the tissue of the cardiac cells, chains of neurons or chemical reactions, and the local denaturation of the DNA double strand [40,41]. Information conduction and convection in noiseless Vicsek flocks [37] has been studied using the two-dimensional (2D) version of the DVM [31,32]. Classical continuum approaches cannot adequately describe high-frequency vibrations, behavior of material near cracks and fronts of destruction waves [38]. McGaughey and Kaviany [44] notice that the thermal transport in dielectrics materials is not localized in space because the frequencies and wave numbers in a crystal are discrete and limited, which cannot be described within the framework of a continuum approach.

In the context of transport phenomena, the paper of Fock [27] (see also comments in Ref. [45]) seems to be the first effort to use the discrete variable approach. Fock considered the one-dimensional (1D) problem of light (photon) diffusion in semi-infinite media and obtained transport equations with corresponding boundary conditions in the discrete form. In the continuum limit, the model of Fock leads to both a classical Fourier equation of parabolic type and a hyperbolic

*sobolev@icp.ac.ru

(telegraph) heat equation. The DVM has been formulated also for the 2D case for one- [31,33] and two-temperature systems [32]. To bridge the gap between the DVM and continuum approaches, two types of the continualization procedure with different invariants have been introduced [30–33,35]. Recently, it has been shown that the dispersion relation even for the simplest version of the discrete heat equation (DE) demonstrates critical high-frequency and short-wavelength behavior [43]. The DVM provides evolution equations in the discrete form both for the temperature and for the heat flux [19,28,30,33–35,39,42], which can be used directly for computer simulations [31]. However, in some cases the DVM allows one to obtain analytical solutions in a relatively simple way [19,20,43]. For example, the DVM predicts a transition from the diffusive controlled to ballistic controlled heat conduction regimes, size-dependent and distance-dependent (local) thermal conductivity, and boundary temperature jumps as functions of the film size for the steady-state heat conduction across nanofilms [19,20]. Clearly, there is a strong need of the generalized version of the DVM to better understand heat transport on ultrashort space and time scales when the process occurs under far from local equilibrium conditions [16,39,34,35]. The generalized DVM will be useful in developing and engineering composite multilayered materials, which have been widely used due to their wide range of applications, especially in thermal management of microelectronics and manufacturing nanoarchitected metamaterials [1,2,8]. The paper is structured as follows. In Sec. II we obtain the generalized DEs, which are able to describe heat conduction in the periodic two- and one-layer systems with allowance for the thermal resistance between the discrete layers. The continuum limit of the DE is discussed in Sec. III. The dispersion relation for the generalized DE has been obtained and analyzed analytically in Sec. IV. In Sec. V we consider the continuum limit of the dispersion relation obtained in Sec. IV. In Sec. VI we discuss the main advantages of the DVM, before we conclude in Sec. VII.

II. DISCRETE HEAT EQUATIONS WITH ALLOWANCE FOR THE INTERFACIAL THERMAL RESISTANCE

A. Discrete heat conduction equation for a periodic two-layer system

1. Discrete variables

First, we consider a periodic structure composed of layers of two different materials indexed *A* and *B* [see Fig. 1(a)]. The thicknesses of the layers are denoted as h_A and h_B , respectively. For example, such a system can serve as a temperon crystal [1]. Each discrete layer indexed by j is characterized by heat capacity $C_j = c_j \rho_j h_j$, where h_j is the length of the layer, c_j is the specific heat, and ρ_j is mass density. It is assumed that the temperature of a discrete layer j , denoted $T_{j,n}$, is constant inside the layer and evolves at the discrete time instants $n = 0, 1, 2, \dots$ due to the heat fluxes across the boundaries of the layer (see Fig. 1). The heat fluxes act during the time step τ between two successive changes of temperature at the discrete instants of time n and $(n + 1)$. This implies that in the discrete representation we can assume that the heat flux, denoted $q_{j-1,j,n+1/2}$, is the average heat

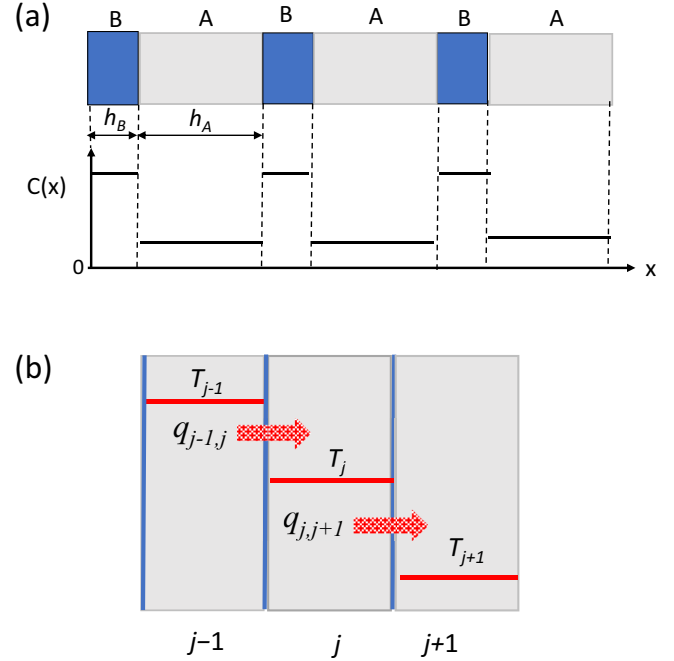


FIG. 1. Schematic representation of the discrete heat conduction model with allowance for the thermal resistance between the discrete layers. (a) Spatially periodic two-layer discrete system: h and l are the thicknesses of the discrete layers. (b) Spatially periodic one-layer discrete system. Temperature of the discrete layers (see red lines) is a volume property. Heat fluxes act through the boundary between the layers (see red arrows), i.e., are a boundary (surface) property.

flux acting through the boundary between the discrete layers ($j-1$) and j at the intermediate instant of time indexed by $(n + 1/2)$ [19,28,30,33–35]. Thus, the energy balance law for the discrete layer j is given by

$$C_j(T_{j,n+1} - T_{j,n}) = (q_{j-1,j,n+1/2} - q_{j,j+1,n+1/2})\tau + Q_{j,n+1/2}, \quad (1)$$

where $q_{j,j+1,n+1/2}$ is the heat flux acting through the boundary between the discrete elements indexed by j and $(j + 1)$ at the instant of time $(n + 1/2)$, and $Q_{j,n+1/2}$ is the heat source. The form of Eq. (1) takes into account that the temperature is a volume property, while the heat flux is a surface property (see Fig. 1).

The heat fluxes across the boundary between the neighboring discrete layers can be represented as follows:

$$q_{j-1,j,n+1/2} = \alpha(T_{j-1,n} - T_{j,n})/\tau, \quad (2)$$

$$q_{j,j+1,n+1/2} = \alpha(T_{j,n} - T_{j+1,n})/\tau, \quad (3)$$

where α is the heat-exchange coefficient between the neighboring discrete layers. The inverse of the heat-exchange coefficients $R = 1/\alpha$ is also referred to as thermal or Kapitza resistance. This definition for the heat fluxes, Eqs. (2) and (3), corresponds to the Newton law of cooling. The term $\alpha T_{j-1,n}$ in Eq. (2) is nothing but the rate of energy flow from the layer ($j-1$) to the layer j , and vice versa, $\alpha T_{j,n}$ is the rate of energy flow from the layer j to the layer ($j-1$). Thus, $q_{j-1,j,n+1/2}$ in Eq. (2) is the net energy flow per unit time between the elements $j-1$ and j , i.e., the heat flux.

Using Eqs. (1)–(3), we obtain the DE with allowance for the boundary resistance between the discrete layers as follows:

$$(T_{j,n+1} - T_{j,n}) = \frac{\beta_j}{2}(T_{j-1,n} - 2T_{j,n} + T_{j+1,n}) + \frac{1}{C_j}Q_{j,n+1/2}, \quad (4)$$

where $\beta_j = 2\alpha/C_j$. For the sake of simplicity, we assume in the following that $Q_{j,n+1/2} = 0$.

2. Continuous variables

Now let us represent Eq. (4) in terms of the continuous variables x and t that are related with the discrete ones as

$$C(x) = \begin{cases} c_B \rho_B h_B; & \text{at } 0 + j(h_A + h_B) < x < j(h_A + h_B) + h_B \\ c_A \rho_A h_A; & \text{at } h_B + j(h_A + h_B) < x < (j+1)(h_A + h_B) \end{cases}, \quad (6)$$

where $j = 0, 1, 2, 3, \dots$ is a number of a discrete layer [see Fig. 1(a)]. Equations (4)–(6) can be directly used for computer simulation of space-time evolution temperature in the periodic discrete multilayered systems, such as temperonic crystals and layered correlated materials [1,2]. However, approximate methods based on Eqs. (4)–(6), that are capable of capturing the ultrashort size and time effects in multilayered systems with allowance for the interfacial resistance but easy to implement analytically are still desired.

B. Discrete heat equation for a periodic one-layer system

1. A periodic one-layer system with allowance for the interfacial thermal resistance

While computational simulations, as discussed above, can be used to solve the discrete equations (4)–(6), they will not replace the analytical approach, which is able to provide physical insights without much numerical effort. In what follows, we are going to slightly simplify Eq. (4) to obtain an analytical expression for the dispersion relation in ω - k space, which readily provides useful information, in particular about attenuation distance, and phase and group velocities. For the sake of simplicity and to present the results analytically, we assume that $h_A \gg h_B$ [see Fig. 1(b)]. In such case, $C_A \gg C_B$ and, consequently, the layers B do not affect the energy balance in the system, but strongly affect the temperature distribution resulting in the thermal resistance between the layers A . Manipulating the physical properties of the layer B and/or its thickness, one can change the value of the interfacial resistance and govern heat conduction regimes in the system. Thus, in what follows, we consider a periodic one-layer system consisting of identical layers A of the same length h [see Fig. 1(b)] and with the same heat capacity $C_j = C$, whereas the heat-exchange coefficient between layers A depends now on the set of thermal properties of the layer B . In such case, Eq. (4) yields

$$T_{j,n+1} - T_{j,n} = \frac{\beta}{2}(T_{j-1,n} - 2T_{j,n} + T_{j+1,n}), \quad (7)$$

follows $x = jh$ and $t = n\tau$. In such case, Eq. (4) takes the form

$$T(x, t + \tau) - T(x, t) = \frac{\beta(x)}{2} \left[T\left(x - \frac{h_A + h_B}{2}, t\right) - 2T(x, t) + T\left(x + \frac{h_A + h_B}{2}, t\right) \right]. \quad (5)$$

Here $\beta(x) = 2\alpha/C(x)$, where $C(x)$ is given by

where $\beta = 2\alpha/C$, $\alpha(c_B, \rho_B, h_B)$ is the heat-exchange coefficient between layers A , which depends on the length and thermal properties of the layer B .

In the continuous variables Eq. (7) takes the form

$$T(x, t + \tau) - T(x, t) = \frac{\beta}{2} [T(x + h, t) - 2T(x, t) + T(x - h, t)]. \quad (8)$$

2. A periodic one-layer system: Probability formulation

The discrete heat equation can be also obtained on the basis of the random-walk approach [27–29]. In the following it is assumed that the energy carriers at the discrete layer j are allowed to move the neighboring layers $(j+1)$ and $(j-1)$, as well as they are allowed to stay at rest. In such case, the discrete heat equation takes the form [43]

$$T_{j,n+1} = p_+ T_{j+1,n} + p_- T_{j-1,n} + p_0 T_{j,n}, \quad (9)$$

where p_- and p_+ are the probability that the energy carrier comes from the discrete layer $(j-1)$ and $(j+1)$, respectively, whereas p_0 is the probability that the energy carrier comes to rest. Conservation law implies that $p_+ + p_- + p_0 = 1$. For the following consideration, we assume the symmetrical case $p_+ = p_- \equiv p$, which gives $p_0 = 1 - 2p$. In such case, Eq. (9) takes the form

$$T_{j,n+1} - T_{j,n} = p(T_{j-1,n} - 2T_{j,n} + T_{j+1,n}), \quad (10)$$

or in terms of the continuous variables

$$T(t + \tau, x) - T(x, t) = p[T(t, x + h) - 2T(x, t) + T(t, x - h)]. \quad (11)$$

A comparison of Eqs. (7) and (10), as well as Eqs. (8) and (11), demonstrates that the thermodynamic approach and random-walk model lead to a similar discrete heat equation. The nondimensional interfacial thermal resistance between the discrete layers β can be expressed in terms of probability as $\beta = 2p$. Taking into account that $p \leq 1/2$, we obtain that $\beta \leq 1$.

III. CONTINUUM LIMIT

A. Discrete equation vs continuous partial differential equations

To bridge the gap between the discrete and continuum approaches, we consider Eq. (8) in the limit $\tau \rightarrow 0$ and $h \rightarrow 0$. The Taylor expansion of the DE, Eq. (8), around $\tau = 0$ and $h = 0$ contains an infinite number of terms with two small parameters τ and h :

$$\sum_{m=1}^{\infty} \frac{\tau^m}{m!} \frac{\partial^m T}{\partial t^m} = \frac{\beta}{2} \left[\sum_{m=2}^{\infty} \left(\frac{h^m}{m!} \frac{\partial^m T}{\partial x^m} + \frac{(-h)^m}{m!} \frac{\partial^m T}{\partial x^m} \right) \right]. \quad (12)$$

To obtain partial differential equations (PDEs) with a finite number of terms, it is necessary to use two types of the continualization procedure, which balances the fast-time τ and short-space h scales in the continuum limit $\tau \rightarrow 0$ and $h \rightarrow 0$ [30–33,35,42,43].

1. Diffusivelike continualization procedure

The first type of continualization procedure assumes that $D = h^2/2\tau$, which plays a role of thermal diffusivity, preserves a finite value when $\tau \rightarrow 0$ and $h \rightarrow 0$ [30–33,35,42,43]. In such case, the first-order approximation of Eq. (12) leads to the classical Fourier equation of parabolic type:

$$\frac{\partial T}{\partial t} = \beta D \frac{\partial^2 T}{\partial x^2}, \quad (13)$$

where βD is the effective thermal diffusivity, which depends on the heat-exchange coefficient β .

The second-order approximation gives

$$\frac{\partial T}{\partial t} + \frac{\tau}{2} \frac{\partial^2 T}{\partial t^2} = \beta D \frac{\partial^2 T}{\partial x^2} + \frac{\beta D h^2}{24} \frac{\partial^4 T}{\partial x^2}. \quad (14)$$

Using Eq. (13), the last term in Eq. (14) can be represented as $\frac{\partial^2}{\partial x^2} \left(\frac{\partial^2}{\partial x^2} \right) = \frac{\partial^2}{\partial x^2} \left(\frac{1}{\beta D} \frac{\partial}{\partial t} \right)$. In such case, Eq. (14) takes the form

$$\frac{\partial T}{\partial t} + \frac{\tau}{2} \frac{\partial^2 T}{\partial t^2} = \beta D \frac{\partial^2 T}{\partial x^2} + \frac{h^2}{24} \frac{\partial^3 T}{\partial x^2 \partial t}. \quad (15)$$

Equation (15) is similar to the 1D Guyer-Krumhansl (GK) equation and Jeffreys type equation [46]. Note that Eqs. (13)–(15) are of parabolic type with an infinite velocity of thermal signal v . Indeed, $v = h/\tau = (D/h) \rightarrow \infty$ when D preserves a finite value and $h \rightarrow 0$.

2. Wavelike continualization procedure

The second invariant of the continualization procedure keeps a finite value of propagation velocity of thermal signal $v = h/\tau$ when $\tau \rightarrow 0$ and $h \rightarrow 0$ [30–33,35,42,43]. In such case, the first-order approximation of Eq. (12) leads to the hyperbolic equation (HE) as follows:

$$\frac{\partial T}{\partial t} + \frac{\tau}{2} \frac{\partial^2 T}{\partial t^2} = \frac{\beta v^2 \tau}{2} \frac{\partial^2 T}{\partial x^2}. \quad (16)$$

Similar to the previous case, the effective thermal diffusivity given by $\beta v^2 \tau/2$ depends on the heat-exchange coefficient β .

3. Some comments

Equation (12) demonstrates that the DE, Eq. (8), contains an infinite hierarchy of the continuous PDEs [42,43]. In particular, the hierarchy includes the parabolic equation (PE), HE, GK, and Jeffreys type equations [see Eqs. (13)–(16)]. This corresponds to the conclusion of Mickens and Washington [36] that “any finite order difference equation corresponds to an infinite order differential equation.” The continualization procedure, which balances the internal fast-time and the short-space scales when they tend to zero, preserves the basic invariant of the process described by the DE [30–33,35,42,43]. The diffusivelike continualization procedure preserves a finite value of thermal diffusivity. This takes into account only the diffusive (dissipative) mode of heat transport but loses the wave mode. The procedure leads to a hierarchy of PDEs of parabolic type with an infinite propagation velocity of thermal disturbances. The wavelike continualization procedure preserves both modes and leads to a hierarchy of PDEs of hyperbolic type with a finite velocity of thermal disturbances. It should be stressed that the PDEs with a finite number of terms, in particular Eqs. (13)–(16), are the truncated Taylor series expansions of the DE and approximate the DE with some accuracy (see also discussion in [36]). The type of PDEs with a finite number of terms, parabolic or hyperbolic, depends on the invariant of the continualization procedure.

To select a suitable approach, i.e., the DE or PDE with a finite number of terms, one should consider the ratios of the internal fast time τ and/or short space h scales to the characteristic time and/or space scales of the process under consideration, respectively. When these ratios are much smaller than unity, the heat transport is purely diffusive, and the classical Fourier PE can be used. When one or both ratios increase but are still smaller than unity, the PDE of higher order is required. The invariant chosen depends on whether the diffusive or the wave mode of heat conduction plays the most important part in the problem of interest. The number of terms in the PDE depends on what accuracy of calculations is required in the analysis. When one or both ratios become comparable to unity, the PDEs with a finite number of terms may result in significant errors and the DE is preferable.

B. Discrete equation vs mixed discrete-continuous heat equation

Using the Taylor series expansion of the left-hand side of the DE, Eq. (8), and keeping the right-hand side in the discrete form, we obtain the mixed discrete-continuous (or difference-differential) equation as follows:

$$\tau \frac{\partial T}{\partial t} + \frac{\tau^2}{2} \frac{\partial^2 T}{\partial t^2} + O(\tau^3) = \frac{\beta}{2} [T(x+h, t) - 2T(x, t) + T(x-h, t)]. \quad (17)$$

Similar mixed difference-differential equations arise in the theory of atomic [47–50] and thermal [51,52] lattice (chains) dynamics, which assume that only space is described by a discrete variable, whereas time is continuous. Keeping the first term on the left-hand side of Eq. (17), one obtains the mixed discrete-continuous equation whose left-hand side corresponds to the classical Fourier law, Eq. (13). Such kind of

equation has been used to study the nonlocal thermal diffusion in a one-dimensional periodic thermal lattice [51]. Taking into account the two first terms on the left-hand side of Eq. (17), one obtains the mixed continuous-discrete equation whose left-hand side corresponds to the continuous HE, Eq. (16). In such case, Eq. (17) with two first terms on the left-hand side can be treated as a spatial discrete formulation of the HE [52].

Equation (17) is similar to the quantum Langevin equation for a harmonic atomic chain without noise term [48,49]. In this case the first-time derivative in the dynamic discrete-continuous equation arises due to friction (dissipation) effects.

Note that the mixed discrete-continuous equations obtained as the truncated Taylor series of the DE around $\tau = 0$ are only approximations of the DE and their solutions may differ significantly when the characteristic time of the process under consideration is of the order of τ . In such case the mixed discrete-continuous equations may lead to erroneous results.

Another type of discrete-continuous equation can be obtained under the assumption that time is discrete, while space is continuous. In this case, the DE, Eq. (8), gives

$$T(x, t + \tau) - T(x, t) = \frac{\beta h^2}{2} \frac{\partial^2 T}{\partial x^2} + O(h^4).$$

The Taylor series expansion of the left-hand side of this equation gives the PE, Eq. (13), as the first-order approximation and the HE, Eq. (16), as the second-order approximation.

IV. DISPERSION ANALYSIS

A. Dispersion relation for the DE

Now we are going to obtain an analytical expression for the dispersion relation of Eq. (8). The dispersion analysis is able to provide important information, such as attenuation distance, and phase and group velocities as functions of the governing parameters [1,2,39,53,54]. We use the standard procedure seeking for a solution of Eq. (8) in the form $T = T_0 \exp[i(\omega t + kx)]$, where ω is the real frequency and k is the complex wave number. In such case, we obtain the dispersion relation for Eq. (8) in the form

$$\exp(i\omega\tau) - 1 = \beta[\cos(kh) - 1]. \quad (18)$$

Equation (18) gives the complex wave number as a function of the frequency as follows:

$$kh = \arccos\left(\frac{\cos(\omega\tau) - 1 + i \sin(\omega\tau)}{\beta} + 1\right). \quad (19)$$

After some algebra (for details, see the Appendix), we obtain analytical expressions for the real and imaginary parts of the wave number in the form

$$\text{Re}kh = \pm \arccos \frac{2[\cos(\omega\tau) + \beta - 1]}{2\beta G} + 2m\pi, \quad (20)$$

$$\text{Im}kh = \pm \ln(G + \sqrt{G^2 - 1}) + i2m\pi, \quad (21)$$

where m is an integer and

$$G = \frac{2 \sin(\omega\tau/2) + \sqrt{1 + (2\beta - 1)^2 + 2(2\beta - 1) \cos(\omega\tau)}}{2\beta}. \quad (22)$$

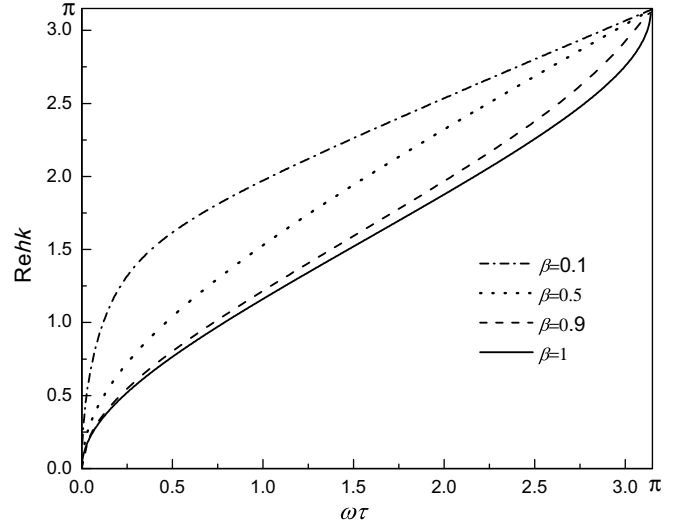


FIG. 2. Real part of the wave number $\text{Re}kh$, Eq. (20), for the DE, Eq. (8), as a function of $\omega\tau$ in the region $0 \leq \omega\tau \leq \pi$ for different values of β .

Figure 2 shows the $\text{Re}kh$, Eq. (20), as a function of $\omega\tau$ for the principal value of arccosine in the region $0 \leq \omega\tau \leq \pi$ at different β (the same function in a wider range of $\omega\tau$ is shown in Supplemental Material (SM) [55]). The $\text{Re}kh$ monotonically increases with increasing $\omega\tau$ for any value of β and reaches its maximum value $\text{Re}kh = \pi$ at the maximum allowed frequency $\omega\tau = \pi$ (see Fig. 2). Similar behavior of the dispersion curve has been observed in the lattice (chain) model [47] and in the two-temperature mass-in-mass chain model [50], where the allowed wave number is restricted by the spacing of the atoms. However, an important distinction between the present DVM and the lattice model is that in Eqs. (7)–(11) both space and time are discrete variables, whereas in the lattice model only the space is discrete but time is a continuous variable. As a consequence, in the discrete model the maximum allowed frequency (or, equivalently, minimum allowed time scale) is limited, whereas in the lattice models there is no any restriction on the frequency.

Figure 3 shows the $\text{Re}kh$ as a function of β at $0 < \beta \leq 1$ for $\omega\tau = \pi/4$, $\omega\tau = \pi/2$, and $\omega\tau = 3\pi/4$. Figure 3 demonstrates that the real part of the wave number, Eq. (20), monotonically decreases with increasing heat-exchange coefficient between the discrete layers β .

Figure 4 shows the $\text{Im}kh$, Eqs. (21) and (22), as a function of the $\omega\tau$ for the principal value of arccosine $0 \leq \omega\tau \leq \pi$ at different β (the same function in a wider range of $\omega\tau$ is shown in the SM). When β is in the region closed to unity, namely, $0.7 \lesssim \beta \leq 1$, the $\text{Im}kh$ first increases with increasing $\omega\tau$, reaches a maximum value at $\omega\tau \approx \pi/2$, and then decreases. For $\beta \lesssim 0.7$, the $\text{Im}kh$ monotonically increases with increasing $\omega\tau$. Note that at $\beta = 1$, $\text{Im}kh \rightarrow 0$ both at $\omega\tau \rightarrow 0$ and at high $\omega\tau \rightarrow \pi$. When $\beta < 1$, $\text{Im}kh \rightarrow 0$ only in the low-frequency limit $\omega\tau \rightarrow 0$, whereas at $\omega\tau \rightarrow \pi$ we obtain that $\text{Im}kh > 0$ (see Fig. 4).

Figure 5 shows the $\text{Im}kh$, Eq. (21), as a function of β at $0 < \beta \leq 1$ for $\omega\tau = \pi/4$, $\omega\tau = \pi/2$, and $\omega\tau = 3\pi/4$. Similar to the $\text{Re}kh$, the $\text{Im}kh$ monotonically decreases with

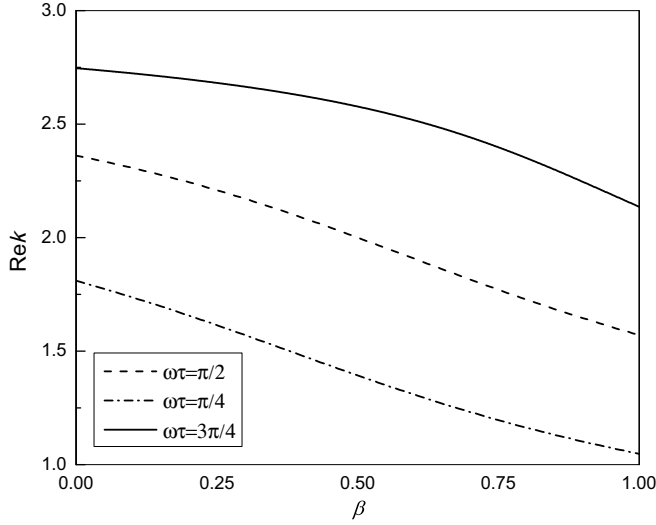


FIG. 3. Real part of the wave number $Re kh$, Eq. (20), as a function of β for $\omega\tau = \pi/4$, $\omega\tau = \pi/2$, and $\omega\tau = 3\pi/4$.

increasing β for all values of $\omega\tau$. However, the values of $Im kh$ for different $\omega\tau$ at a given value of β are significantly smaller than the values of $Re kh$ (compare Figs. 3 and 5).

B. Special case $\beta = 1$

Let us consider a special case $\beta = 1$, which, as discussed above, corresponds to $p = 1/2$ and $p_0 = 0$. In such case, both Eq. (7) and Eq. (11) reduce to [28–30,39]

$$T_{j,n+1} = \frac{1}{2}(T_{j-1,n} + T_{j+1,n}).$$

This equation implies that all the energy carriers move out of a layer j through the boundaries with neighboring layers. In other words, this can be treated as an absence of interfacial thermal resistance. The corresponding dispersion relation is given by [39]

$$\exp(i\omega\tau) = \cos(kh).$$

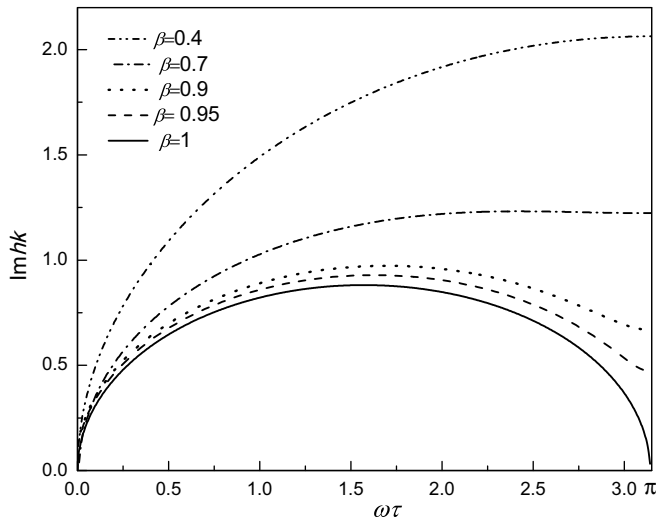


FIG. 4. Imaginary part of the wave number $Im kh$, Eq. (21), as a function of $\omega\tau$ at different β .

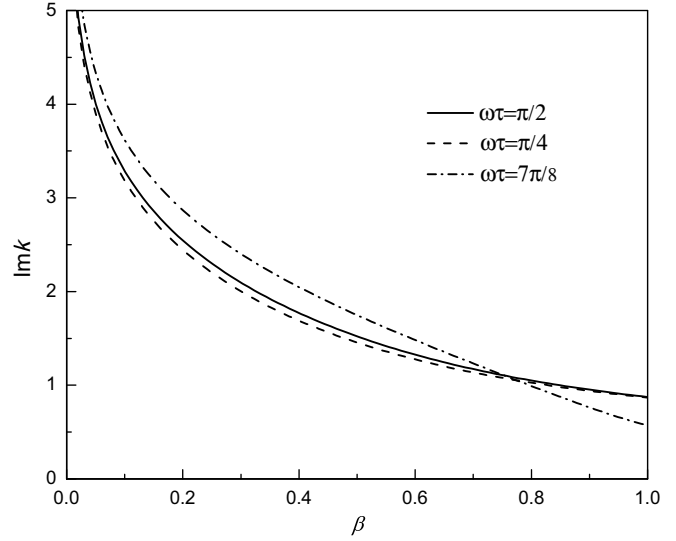


FIG. 5. Imaginary part of the wave number $Im kh$, Eq. (21), as a function of β at $0 < \beta \leq 1$ for $\omega\tau = \pi/4$, $\omega\tau = \pi/2$, and $\omega\tau = 3\pi/4$.

The real and imaginary parts of the wave vector as functions of frequency can be obtained from Eqs. (20) and (21), respectively, and are given by [39]

$$Re kh = \pm\{\arccos[\cos(\omega\tau/2) - \sin(\omega\tau/2)] + 2m\pi\},$$

$$Im kh = \pm\{\ln[\sin(\omega\tau/2) + \cos(\omega\tau/2) + \sqrt{\sin(\omega\tau)}]\} + i2m\pi.$$

The behavior of the $Re kh$ and $Im kh$ at $\beta = 1$ as functions of frequency is shown in Figs. 2 and 4, respectively.

C. Phase and group velocities

Phase velocity and group velocity are defined as $v_p = \omega/Re k$ and $v_g = \partial\omega/\partial Re k$, respectively. Figure 6 shows the

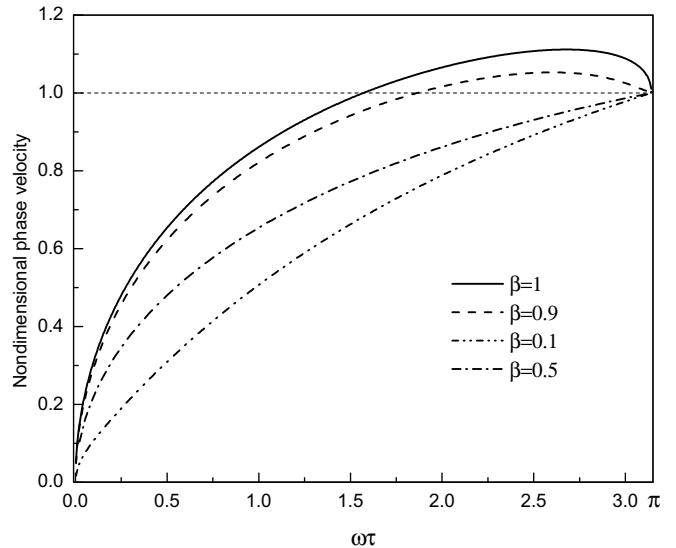


FIG. 6. Nondimensional phase velocity v_p/v as a function of $\omega\tau$ for different β .

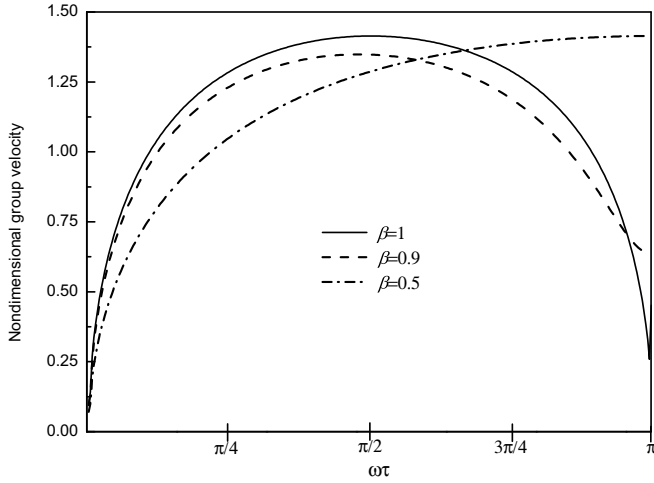


FIG. 7. Nondimensional group velocity v_g/v as a function of $\omega\tau$ for different β .

behavior of the phase velocity as a function of $\omega\tau$ for $0.5 < \beta \leq 1$ calculated from Eq. (20). The nondimensional phase velocity v_p/v exceeds unity at a relatively high frequency $\omega\tau > 1.5$, whereas at $\beta < 0.5$ the ratio v_p/v is less than unity at any frequency. The small values of β decrease the energy exchange between the layers, which in turn decreases the phase velocity.

Figure 7 shows the behavior of the group velocity as a function of $\omega\tau$ for $\beta = 1; 0.9; 0.5$ calculated from Eq. (21). When $\beta = 1$, the group velocity v_g equals zero both at $\omega\tau \rightarrow 0$ and $\omega\tau \rightarrow \pi$. At $\beta < 1$, $v_g \rightarrow 0$ only in the low-frequency limit $\omega\tau \rightarrow 0$, whereas in the high-frequency limit $\omega\tau \rightarrow \pi$, we obtain that $v_g > 0$ (see Fig. 7).

D. Attenuation distance

The temperature oscillation can be represented as

$$T(x, t) = T_0 \exp\{i[\omega t + x(\text{Re}k + i \text{Im}k)]\},$$

where $\text{Re}k(\omega\tau)$ and $\text{Im}k(\omega\tau)$ are given by Eqs. (11) and (12), respectively. After some algebra, we obtain

$$T(x, t) = T_0 [\cos(\omega t + x \text{Re}k) + i \sin(\omega t + x \text{Re}k)] \times \exp(-x \text{Im}k).$$

This equation gives the real part of temperature $T(x, t)$ as follows:

$$\text{Re}T(x, t) = T_0 [\cos(\omega t + x \text{Re}k)] \exp(-x \text{Im}k).$$

This equation implies that $\gamma \equiv 1/\text{Im}k$ is an attenuation distance, whereas $\varphi \equiv x \text{Re}k(\omega\tau)$ is a phase lag, i.e., the phase difference between oscillations at a point x and the boundary $x = 0$ where $\text{Re}T(0, t) = T_0 \cos(\omega t)$. Figure 8 shows the attenuation distance γ as a function of $\omega\tau$ for different values of β .

V. CONTINUUM LIMIT OF THE DISPERSION RELATION

Now let us consider the dispersion relation, Eq. (18), for the DE, Eq. (8), in the continuum limit $\omega\tau \rightarrow 0$ and $kh \rightarrow 0$.

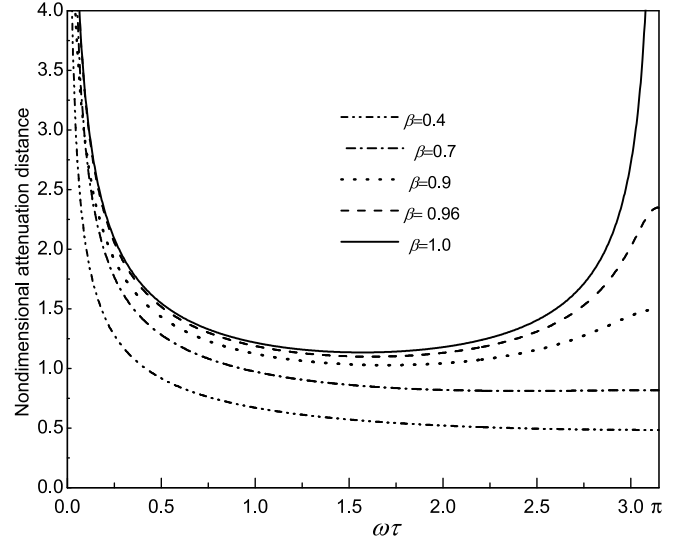


FIG. 8. Attenuation distance γ/h as a function of $\omega\tau$ for different β .

In such case Eq. (18) gives

$$\sum_{m=1}^{\infty} \frac{(i\omega\tau)^m}{m!} = \beta \sum_{m=1}^{\infty} \frac{(kh)^{2m}}{(2m)!}. \quad (23)$$

A. Diffusivelike continualization procedure

The first-order approximation of Eq. (23) results in

$$i\omega\tau = \beta \frac{(kh)^2}{2}. \quad (24)$$

The dispersion relation (24) corresponds to the PE (classical Fourier law), Eq. (11). Using Eq. (24), we obtain

$$kh = \pm \left(\frac{2i\omega\tau}{\beta} \right)^{1/2} = \pm \left(\frac{\omega\tau}{\beta} \right)^{1/2} (1 + i). \quad (25)$$

Equation (25) leads to

$$\text{Re}kh = \text{Im}kh = \left(\frac{\omega\tau}{\beta} \right)^{1/2}. \quad (26)$$

Figure 9 shows the $\text{Re}kh = \text{Im}kh$, Eq. (26), as a function of $\omega\tau$.

Corresponding phase and group velocities and attenuation distance are given by

$$\frac{v_p}{v} = \frac{\omega}{\text{Re}k} = (\omega\tau\beta)^{1/2}, \quad \frac{v_g}{v} = \frac{d\omega}{d \text{Re}k} = 2(\omega\tau\beta)^{1/2},$$

$$\frac{\gamma}{h} = \left(\frac{\beta}{\omega\tau} \right)^{1/2}.$$

Using Eq. (23), we obtain the second-order dispersion relation as follows:

$$i\omega\tau + \frac{(i\omega\tau)^2}{2} = \beta \left[\frac{(kh)^2}{2} + \frac{(kh)^4}{24} \right], \quad (27)$$

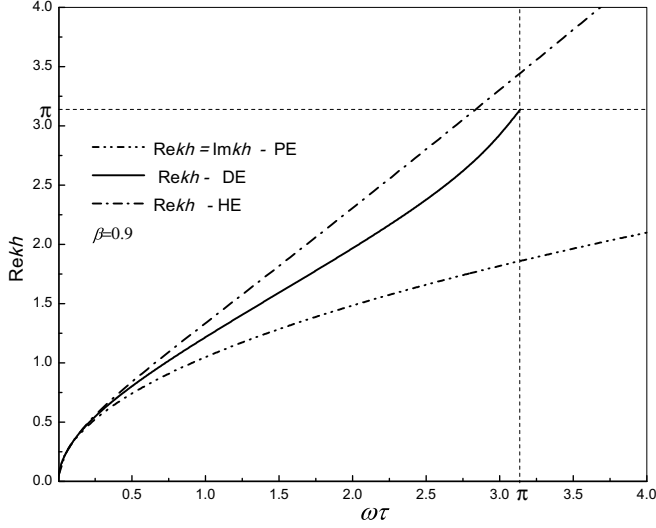


FIG. 9. Real part of the wave number for the dispersion relations of the continuous PE, Eq. (26) (dash-dot-dot curve), continuous HE, Eq. (33) (dash-dot curve), and the DE, Eq. (20) (solid curve) as functions of normalized frequency $\omega\tau$ for $\beta = 0.9$.

which gives

$$kh = \pm \left\{ \frac{-\beta \pm [\beta^2 - 2\beta(i\omega\tau - \omega^2\tau^2/2)/3]^{1/2}}{\beta/6} \right\}^{1/2}. \quad (28)$$

Equation (28) represents the wave number as a function of frequency with allowance for the second-order terms in the Taylor series expansion, Eq. (23). Using Eq. (24), one can represent Eq. (27) as follows:

$$i\omega\tau + \frac{(i\omega\tau)^2}{2} = \frac{(kh)^2}{2} \left[\beta + \frac{i\omega\tau}{6} \right]. \quad (29)$$

Equation (29) leads to

$$kh = \pm \left[\frac{\omega^2\tau^2(1/3 - \beta) + i\omega\tau(2\beta + \omega^2\tau^2/6)}{\beta^2 + \omega^2\tau^2/36} \right]^{1/2}. \quad (30)$$

Equation (30) is the dispersion relation for the GK or Jeffreys type equation. A dispersion relation for the equation similar to the GK or Jeffreys type equation has been discussed in [53].

B. Wavelike continualization procedure

The first-order approximation of Eq. (21) in the wavelike continuum limit yields

$$i\omega\tau + \frac{(i\omega\tau)^2}{2} = \frac{\beta(kh)^2}{2}, \quad (31)$$

which corresponds to the HE, Eq. (13). Equation (31) leads to the dispersion relation in the form

$$kh = \pm \left(\frac{2i\omega\tau - \omega^2\tau^2}{\beta} \right)^{1/2}. \quad (32)$$

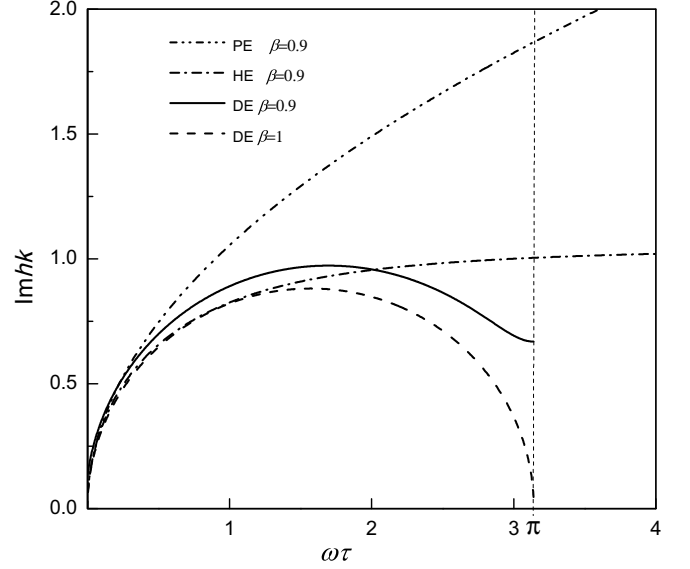


FIG. 10. Imaginary part of the wave number for the dispersion relations of the continuous PE, Eq. (26) (dash-dot-dot curve), continuous HE, Eq. (34) (dash-dot curve), and the DE, Eq. (21) (solid curve) as functions of normalized frequency $\omega\tau$ for $\beta = 0.9$. Dashed curve: the imaginary part of the DE, Eq. (21), for $\beta = 1$.

Equation (32) gives

$$\text{Re}kh = \pm \left[\frac{(\omega^4\tau^4 + 4\omega^2\tau^2)^{1/2} - \omega^2\tau^2}{2\beta} \right]^{1/2}, \quad (33)$$

$$\text{Im}kh = \pm \left[\frac{(\omega^4\tau^4 + 4\omega^2\tau^2)^{1/2} + \omega^2\tau^2}{2\beta} \right]^{1/2}. \quad (34)$$

Figures 9 and 10 show $\text{Re}kh$, Eq. (33), and $\text{Im}kh$, Eq. (34), as functions of normalized frequency $\omega\tau$.

Using Eq. (33), we obtain the phase and group velocities as follows:

$$\frac{v_p}{v} = \frac{\omega}{v \text{Re}k} = \left[\frac{2\beta\omega^2\tau^2}{(\omega^4\tau^4 + 4\omega^2\tau^2)^{1/2} + \omega^2\tau^2} \right]^{1/2},$$

$$\frac{v_g}{v} = \frac{1}{v} \frac{d\omega}{d \text{Re}k} = \frac{2[\beta \sin(\omega\tau)]^{1/2}}{\sin(\omega\tau/2) + \cos(\omega\tau/2)}.$$

Equation (34) gives the attenuation distance γ in the form

$$\frac{\gamma}{h} = \frac{1}{\text{Im}kh} = \left[\frac{2\beta}{(\omega^4\tau^4 + 4\omega^2\tau^2)^{1/2} + \omega^2\tau^2} \right]^{1/2}.$$

Note that $\text{Re}kh$, $\text{Im}kh$, v_p , v_g , and γ for the continuous PDEs are defined in the region $0 \leq \omega\tau < \infty$.

C. Comparison with the spectrum of the DE

First, let us recall that the continuous PE and HE are the truncated Taylor series expansions of the DE at small frequencies and, consequently, cannot approximate the DE quite well at a high frequency. Figures 9 and 10 compare the spectra of the continuous PE and HE with the spectrum of the DE and confirm this conclusion. At small frequencies, the characteristic time of the process under consideration is

much larger than τ and the dissipative mode dominates over the wave (propagative) mode. This implies that the spectra of the continuous PE and HE, as well as the DE, are purely diffusive and match each other. However, at higher frequencies the spectra deviate significantly. Moreover, the allowed values of the frequency and the wave number for the spectrum of the DE are limited due to the discrete structure of the DE, whereas the spectra of the continuous PDEs are not (see Figs. 9 and 10).

At a moderate frequency the spectrum of the HE approximates the spectrum of the DE better than the spectrum of the PE (see Figs. 9 and 10). The fact is that the HE, as well as the DE, incorporates the fast-time scale τ , which takes into account the wave mode of heat transport, whereas the PE takes into account only the diffusive mode and ignores the wave mode. As the frequency increases, the wave effects begin to play a role and the HE approximates the spectrum of the DE better than the PE. However, despite the fact the HE extends the domain of applicability of the PE from small frequencies to relatively moderate ones, it still cannot be used at high frequencies when the characteristic time scale of the process begins to be comparable to the fast-time scale τ . In such case, the spectral behavior of the HE and DE is completely different (see Figs. 9 and 10) and the HE being the truncated Taylor series expansion of the DE may lead to physically doubtful solutions. A more detailed analysis of the spectra of the continuous PDEs in comparison to the spectrum of the DE for the special case $\beta = 1$ can be found in [39].

A comparison of the attenuation distance obtained from the DE and the PDEs is shown in the SM for different values of β .

VI. ADVANTAGES OF THE DISCRETE APPROACH

An important feature of the discrete approach is that it includes into consideration additional fast-time scale τ and short-space scale h , which are associated with the MFT and MFP of energy carriers, respectively. This takes into account an inherent space-time nonlocality of the transfer process, which begins to play a crucial role when the characteristic space and/or time scales of the process under consideration are of the order of h and/or τ , respectively. The discrete approach leads to evolution equations for the temperature and the heat flux in purely discrete form, which can be used directly for computer simulations. In the framework of the discrete approach the boundary and interfacial conditions receive more precise physical meaning and adequate formulations compared to the continuum approach [19,20,27–29]. The structure of the DE implies a finite propagation velocity of thermal signal and guarantees positiveness of solutions. The additional discrete space-time scales restrict the maximum allowed frequency and wave vector in the dispersion analysis. There are no such limits in a continuum description.

The DE contains an infinite hierarchy of the continuous PDEs including the classical Fourier law, hyperbolic heat equation, and GK (or Jeffreys type) equation. The continuous PDEs are the truncated Taylor series expansions of the DE and approximate the DE with some accuracy. The equation, DE or PDE, chosen to describe a particular heat conduction process depends on the relations between the internal scales, i.e., h and τ , and corresponding external (macro) scales of the

process, respectively, and what level of accuracy is required in the analysis. Generally, the DE equation is superior for simulations of heat transport on ultrashort space-time scales. However, corresponding truncated Taylor series expansions in the form of PDEs may be used to study relatively small frequency situations.

Another advantage of the discrete approach over the continuum one is that only boundary and initial conditions for the temperature are required to obtain solutions of the DE [31,36]. However, the PDEs require knowledge of additional time and spatial (or mixed) derivatives along with initial and boundary conditions for the temperature. Thus, mathematical solutions of the PDEs require additional information that cannot be physically determined [36].

As discussed above, the HE, as well as the GK or Jeffreys type equation, approximates the DE quite well at a relatively moderate frequency when the MFT is still less than the characteristic time scale of the process. At higher frequencies, when the characteristic time scale of the process is of the order of τ , the spectrum of the HE, as well as the GK or Jeffreys type equation, deviates significantly from that of the DE (see Figs. 9 and 10) and the continuous PDEs may lead to physically doubtful solutions.

In addition, the DVM is able to describe the boundary temperature jumps [19–25] and the transition from the diffusive to ballistic modes of heat transport [19–25], which arise on ultrashort space-time scales. The boundary temperature jump occurs, for example, in the nanosized system between the thermostatted and nonthermostatted regions [19,20], which can be treated as a consequence of thermal boundary resistance. Numerical methods such as finite element analysis to study heat conduction problems usually assume that the temperature and heat flux are continuous functions. However, the temperature jumps invalidate the continuity condition of temperature at the interface and result in both larger calculation error and longer simulation time in molecular dynamics (MD) simulations [22], while the DVM copes with the jumps quite well [19,20]. Moreover, the DVM predicts that the local thermal conductivity in nanofilms is position dependent and introduces into consideration the thermal extrapolation length, which virtually eliminates the temperature jump at the boundaries with thermal baths [19]. Thus, the DVM can be used as an effective tool for preliminary calculations to make a more elaborate MD approach less computationally expensive.

Now let us briefly comment about the definition of temperature for the discrete systems. According to Cahill *et al.* [56] “the question ‘What is Temperature?’ is really a question about the size of the regions over which a local temperature can be defined.” Indeed, the classical definition is entirely local, and one can define a temperature for each space point. The DVM assumes that inside the discrete layers the temperature does not change and the thickness of the layers h is the minimum size of the region over which the temperature can be defined. Majumdar [57] seems to be the first to conclude that “a meaningful temperature can be defined only at points separated on an average by the phonon MFP.” This agrees with the statement of Cahill *et al.* [56] that “a local region with a designated temperature must be larger than the phonon scattering distance” (which is of the order

of MFP). The idea corresponds to the concept of a minimum heat affected region suggested by Chen [58], which assumes that during phonon transport from a nanoscale heat source the minimum size of the heat affected region is of the order of the MFP. In addition to these limitations, the DVM also assumes that the minimum size of the heat source acting in the systems is defined by the discrete internal scale h [see Eq. (4)]. Note that the DVM also assumes that for the homogeneous systems the minimum discrete scale h corresponds to the MFP. However, for the multilayer materials the scale h can be associated with the thickness of the layers if the temperature gradient in the layers is relatively small. The reader interested in a detailed definition of temperature on short-space and time scales when the heat conduction occurs under far from local equilibrium conditions is referred to in Refs. [34,35,50,59,60].

In addition, the DVM casts some doubts about the overshooting phenomena [29], which appears as the solutions of the continuous HE and dual-phase-lag (DPL) model on the fast-time scale [61] when the continuous PDEs, as discussed above, reach their limit. Note that the so-called DPL model lacks any evidence of physical or mathematical justification and is nothing but an already existing Jeffreys type or GK equation [46,62,63].

VII. CONCLUSION

DEs for the periodic one- and two-layer systems with allowance for the thermal resistance between the layers have been obtained introducing into consideration two additional internal fast-time and short-space scales. The scales are associated with the MFT and MFP of energy carriers, respectively, and take into account the inherent space-time nonlocality of the transfer process. Based on the dispersion relation for the DE for the one-layer periodic system, we derive analytical expressions for the real and imaginary parts of the wave number, attenuation distance, and phase and group velocities as functions of the frequency and thermal resistance between the layers. In contrast to a continuum description, the maximum allowed angular frequency and wave number for the DE are limited. The dispersion analysis provides a straightforward, easy-to-adopt, analytical tool to investigate different heat conduction regimes, in particular the temperature wave-like phenomena, arising in metamaterials on the ultrashort space-time scales.

Furthermore, it is shown that the DE contains an infinite hierarchy of the continuous PDEs including the classical Fourier law of parabolic type (PE), hyperbolic HE, and Guyer-Krumhansl (or Jeffreys type) equation. To obtain PDEs with a finite number of terms, we use continualization procedures that balance internal fast-time and short-space scales to preserve the main invariant (diffusive or wave) of the original process described by the DE. The continuous PDEs with a finite number of terms approximate the DE quite well only in the low-frequency limit. At a moderate frequency, the HE approximates the spectrum of the DE better than the PE. However, at high frequency, the spectrum of the DE and the spectra of the continuous PDEs differ significantly. This implies that

the continuum approach reaches its limit on the fast-time and short-space scales at which the DE is preferable.

The approach may be of interest for the design of nanoscale thermal devices and metamaterials operating on ultrafast-time and ultra-short-space scales, in particular for the case of quantum materials and graphite.

ACKNOWLEDGMENTS

This work was performed as a part of the State Task of Russian Federation, State Registration No. 124013000760–0.

APPENDIX

Equation (19) can be represented as follows:

$$kh = \arccos(z + iy), \quad (\text{A1})$$

where

$$z = \frac{\cos(\omega\tau) - 1}{\beta}, \quad (\text{A2})$$

$$y = \frac{\sin(\omega\tau)}{\beta}. \quad (\text{A3})$$

Taking into account that $y > 0$ for the principal value of the arccosine between 0 and π , Eqs. (A1)–(A3) lead to [64]

$$kh = \pm \left(\arccos \frac{2z}{p+q} + 2m\pi - i \operatorname{arch} \frac{p+q}{2} \right), \quad (\text{A4})$$

where m is an integer and

$$p = \sqrt{\left(\frac{\cos \omega\tau + 2\beta - 1}{\beta} \right)^2 + \left(\frac{\sin \omega\tau}{\beta} \right)^2}, \quad (\text{A5})$$

$$q = \sqrt{\left(\frac{1 - \cos \omega\tau}{\beta} \right)^2 + \left(\frac{\sin \omega\tau}{\beta} \right)^2}. \quad (\text{A6})$$

Equation (A4) gives the real and imaginary parts of the wave vector as follows:

$$\operatorname{Re}kh \pm \left(\arccos \frac{2z}{p+q} + 2m\pi \right), \quad (\text{A7})$$

$$\operatorname{Im}kh = \mp \left(\operatorname{arch} \frac{p+q}{2} \right). \quad (\text{A8})$$

Equations (A5) and (A6) can be represented as

$$p = \frac{1}{\beta} \sqrt{1 + (2\beta - 1)^2 + 2(2\beta - 1) \cos \omega\tau}, \quad (\text{A9})$$

$$q = \frac{2}{\beta} \sqrt{\frac{1 - \cos \omega\tau}{2}} = \frac{2}{\beta} \sin \frac{\omega\tau}{2}, \quad (\text{A10})$$

which gives

$$p + q = \frac{1}{\beta} \left(\sqrt{1 + (2\beta - 1)^2 + 2(2\beta - 1) \cos \omega\tau} + 2 \sin \omega\tau / 2 \right). \quad (\text{A11})$$

Thus, using Eqs. (A7)–(A11), we obtain

$$\operatorname{Re}kh = \pm \arccos \frac{2(\cos \omega\tau + \beta - 1)}{2 \sin \omega\tau/2 + \sqrt{1 + (2\beta - 1)^2 + 2(2\beta - 1) \cos \omega\tau}} + 2m\pi, \quad (\text{A12})$$

$$\operatorname{Im}kh = \mp \operatorname{arch} \frac{2 \sin \omega\tau/2 + \sqrt{1 + (2\beta - 1)^2 + 2(2\beta - 1) \cos \omega\tau}}{2\beta}. \quad (\text{A13})$$

Equation (A13) can be represented as [64]

$$\operatorname{Arch}G = \pm \ln(G + \sqrt{G^2 - 1}) + i2m\pi, \quad (\text{A14})$$

where G is given by Eq. (22). Equations (A12)–(A14) lead to Eqs. (20) and (21).

-
- [1] M. Gandolfi, C. Giannetti, and F. Banfi, Temperonic crystal: A superlattice for temperature waves in graphene, *Phys. Rev. Lett.* **125**, 265901 (2020).
- [2] G. Mazza, M. Gandolfi, M. Capone, F. Banfi, and C. Giannetti, Thermal dynamics and electronic temperature waves in layered correlated materials, *Nat. Commun.* **12**, 6904 (2021).
- [3] M. Xu, Nonlocal heat conduction in silicon nanowires and carbon nanotubes, *Heat Mass Transfer* **57**, 843 (2021).
- [4] M. Xu, A non-local constitutive model for nano-scale heat conduction, *Int. J. Therm. Sci.* **134**, 594 (2018).
- [5] H.-L. Li, Y.-C. Hua, and B.-Y. Cao, A hybrid phonon Monte Carlo-diffusion method for ballistic-diffusive heat conduction in nano- and micro- structures, *Int. J. Heat Mass Transfer* **127**, 1014 (2018).
- [6] W. Liu, K. Saanouni, S. Forest, and P. Hu, The micromorphic approach to generalized heat equations, *J. Non-Equilib. Thermodyn.* **42**, 327 (2017).
- [7] R. A. El-Nabulsi, Nonlocal approach to nonequilibrium thermodynamics and nonlocal heat diffusion processes, *Continuum Mech. Thermodyn.* **30**, 889 (2018).
- [8] A. Beardo *et al.*, Observation of second sound in a rapidly varying temperature field in Ge, *Sci. Adv.* **7**, eabg4677 (2021).
- [9] C. Li, X. Tian, and T. He, Size-dependent buckling analysis of Euler-Bernoulli nanobeam under non-uniform concentration, *Arch. Appl. Mech.* **90**, 1845 (2020).
- [10] F. Wang, K. Zhang, and B. Zheng, The non-local effects induced by rapid transient mass diffusion in a spherical silicon electrode of lithium-ion batteries, *Acta Mech. Solida Sin.* **35**, 174 (2022).
- [11] C. Li, H. Guo, X. Tian, and T. He, Nonlocal diffusion-elasticity based on nonlocal mass transfer and nonlocal elasticity and its application in shock-induced responses analysis, *Mech. Adv. Mater. Struct.* **28**, 827 (2019).
- [12] H. Guo, T. He, X. Tian, and F. Shang, Size-dependent mechanical-diffusion responses of multilayered composite nanoplates, *Waves Random Complex Media* **31**, 2355 (2021).
- [13] H. Guo, Y. Lu, F. Shang, and T. He, Nonlocal mechanical-diffusion model with Eringen-type nonlocal single-phase-lag mass transfer and its application in structural dynamics response of a thin nanoplate, *Waves Random and Complex Media* (Taylor & Francis, New York, 2022), pp. 1–24.
- [14] K. Kosmidis and G. Dassios, Monte Carlo simulations in drug release, *J. Pharmacokinet. Pharmacodyn.* **46**, 165 (2019).
- [15] M. Čukić and S. Galovic, Mathematical modeling of anomalous diffusive behavior in transdermal drug-delivery including time-delayed flux concept, *Chaos, Solitons Fractals* **172**, 113584 (2023).
- [16] S. L. Sobolev, Local nonequilibrium electron transport in metals after femtosecond laser pulses: A multi-temperature hyperbolic model, *Nanoscale Microscale Thermophys. Eng.* **25**, 153 (2021).
- [17] A. I. Zhmakin, *Non-Fourier Heat Conduction* (Springer, Cham, 2023).
- [18] R. Kovacs, Heat equations beyond Fourier: From heat waves to thermal metamaterials, *Phys. Rep.* **1048**, 1 (2024).
- [19] S. L. Sobolev and I. Kudinov, Heat conduction across 1D nano film: Local thermal conductivity and extrapolation length, *Int. J. Therm. Sci.* **159**, 106632 (2021).
- [20] S. L. Sobolev, Bing-Yang Cao, and I. V. Kudinov, Non-Fourier heat transport across 1D nano film between thermal reservoirs with different boundary resistances, *Physica E (Amsterdam, Neth.)* **128**, 114610 (2021).
- [21] J. Ordonez-Miranda, R. Yang, S. Volz, and J. J. Alvarado-Gil, Steady state and modulated heat conduction in layered systems predicted by the analytical solution of the phonon Boltzmann transport equation, *J. Appl. Phys.* **118**, 075103 (2015).
- [22] J.-W. Jiang, J. Chen, J.-S. Wang, and B. Li, Edge states induce boundary temperature jump in molecular dynamics simulation of heat conduction, *Phys. Rev. B* **80**, 052301 (2009).
- [23] T. Xue, X. Zhang, and K. K. Tamma, On a generalized non-local two-temperature heat transfer DAE modeling/simulation methodology for metal-nonmetal thermal interfacial problems, *Int. J. Heat Mass Transfer* **138**, 508 (2019).
- [24] M. G. Hennessy, M. Calvo-Schwarzwalder, and T. G. Myers, Modelling ultra-fast nanoparticle melting with the Maxwell-Cattaneo equation, *Appl. Math. Modell.* **69**, 201 (2019).
- [25] M. Calvo-Schwarzwalder, T. G. Myers, and M. G. Hennessy, The one-dimensional Stefan problem with non-Fourier heat conduction, *Int. J. Thermal Sci.* **150**, 106210 (2020).
- [26] F. Vazquez, M. Lopez de Haro, and A. Figueroa, On the causality relations in thermoelectricity, *Continuum Mech. Thermodyn.* **30**, 1201 (2018).
- [27] V. A. Fock, The solution of a problem of diffusion theory by the method of finite differences and its application to the diffusion of light, *Trans. Opt. Inst., Leningrad* **4**, 1 (1926).
- [28] Ya B. Zeldovich and A. D. Myskis, *Elements of Mathematical Physics* (Nauka, Moscow, 1973).

- [29] Y. Taitel, On the parabolic, hyperbolic, and discrete formulation of the heat conduction equation, *Int. J. Heat Mass Transfer* **15**, 369 (1972).
- [30] S. L. Sobolev, Transport processes and traveling waves in systems with local nonequilibrium, *Sov. Phys. Usp.* **34**, 217 (1991).
- [31] S. L. Sobolev, Discrete model for transfer processes, *Phys. Lett. A* **163**, 101 (1992).
- [32] S. L. Sobolev, Two-temperature discrete model for nonlocal heat conduction, *J. Phys. III* **3**, 2261 (1993).
- [33] S. L. Sobolev, Equations of transfer in non-local media, *Int. J. Heat Mass Transfer* **37**, 2175 (1994).
- [34] S. L. Sobolev, Effective temperature in nonequilibrium state with heat flux using discrete variable model, *Phys. Lett. A* **381**, 2893 (2017).
- [35] S. L. Sobolev, Hyperbolic heat conduction, effective temperature, and third law for nonequilibrium systems with heat flux, *Phys. Rev. E* **97**, 022122 (2018).
- [36] R. Mickens and T. Washington, Construction and analysis of a discrete heat equation using dynamic consistency: The meso-scale limit, *Appl. Numer. Math.* **199**, 114 (2024).
- [37] D. Geiß, K. Kroy, and V. Holubec, Information conduction and convection in noiseless Vicsek flocks, *Phys. Rev. E* **106**, 014609 (2022).
- [38] I. V. Andrianov, J. Awrejcewicz, and D. Weichert, Improved continuous models for discrete media, *Math. Probl. Eng.* **2010**, 986242 (2010).
- [39] S. L. Sobolev, Discrete heat conduction equation: Dispersion analysis and continuous limits, *Int. J. Heat Mass Transfer* **221**, 125062 (2024).
- [40] P. G. Kevrekidis and I. G. Kevrekidis, Heterogeneous versus discrete mapping problem, *Phys. Rev. E* **64**, 056624 (2001).
- [41] P. G. Kevrekidis, I. G. Kevrekidis, A. R. Bishop, and E. S. Titi, Continuum approach to discreteness, *Phys. Rev. E* **65**, 046613 (2002).
- [42] S. L. Sobolev, Local non-equilibrium transport models, *Usp. Fiz. Nauk.* **167**, 1095 (1997); *Phys.-Usp.* **40**, 1043 (1997).
- [43] O. Zobiri, A. Atia, and M. Arıcı, Mesoscale investigation of specularly parameter impact on heat transport in graphene nanoribbon, *Physica E (Amsterdam, Neth.)* **139**, 115153 (2022).
- [44] A. J. H. McGaughey and M. Kaviani, Phonon transport in molecular dynamics simulations: Formulation and thermal conductivity prediction, *Adv. Heat Transfer* **39**, 169 (2006).
- [45] S. L. Sobolev, On hyperbolic heat-mass transfer equation, *Int. J. Heat Mass Transfer* **122**, 629 (2018).
- [46] D. D. Joseph and L. Preziosi, Heat waves, *Rev. Mod. Phys.* **61**, 41 (1989).
- [47] M. T. Dove, Introduction to the theory of lattice dynamics, *Collection SFN* **12**, 123 (2011).
- [48] D. Roy, Crossover from ballistic to diffusive thermal transport in quantum Langevin dynamics study of a harmonic chain connected to self-consistent reservoirs, *Phys. Rev. E* **77**, 062102 (2008).
- [49] D. Segal, Absence of thermal rectification in asymmetric harmonic chains with self-consistent reservoirs, *Phys. Rev. E* **79**, 012103 (2009).
- [50] S. D. Liazhkov and V. A. Kuzkin, Unsteady two-temperature heat transport in mass-in-mass chains, *Phys. Rev. E* **105**, 054145 (2022).
- [51] V. Picandet and N. Challamel, Nonlocal thermal diffusion in one-dimensional periodic lattice, *Int. J. Heat Mass Transfer* **180**, 121753 (2021).
- [52] E. Nuñez del Prado, N. Challamel, and V. Picandet, Discrete and nonlocal solutions for the lattice Cattaneo-Vernotte heat diffusion equation, *Math. Mech. Complex Syst.* **9**, 367 (2021).
- [53] M. Gandolfi, G. Benetti, C. Glorieux, C. Giannetti, and F. Banfi, Accessing temperature waves: A dispersion relation perspective, *Int. J. Heat Mass Transfer* **143**, 118553 (2019).
- [54] D. Zhang and M. Ostoja-Starzewski, Telegraph equation: Two types of harmonic waves, a discontinuity wave, and a spectral finite element, *Acta Mech.* **230**, 1725 (2019).
- [55] See Supplemental Material at <http://link.aps.org/supplemental/10.1103/PhysRevE.109.054102> for shows the real and imaginary parts of the wave number in a wide frequency range.
- [56] D. G. Cahill, W. K. Ford, K. E. Goodson, G. D. Mahan, A. Majumdar, H. J. Maris, R. Merlin, and S. R. Phillpot, *J. Appl. Phys.* **93**, 793 (2003).
- [57] A. Majumdar, Microscale heat conduction in dielectric thin films, *J. Heat Transfer* **115**, 7 (1993).
- [58] G. Chen, Nonlocal and nonequilibrium heat conduction in the vicinity of nanoparticles, *J. Heat Transfer* **118**, 539 (1996).
- [59] S. L. Sobolev and I. V. Kudinov, Ordered motion of active colloids and effective temperature, *Physica A (Amsterdam, Neth.)* **540**, 123155 (2020).
- [60] S. L. Sobolev and I. V. Kudinov, Extended nonequilibrium variables for 1D hyperbolic heat conduction, *J. Non-Equilib. Thermodyn.* **45**, 209 (2020).
- [61] Y. J. Yu, C.-L. Li, Z.-N. Xue, and X.-G. Tian, The dilemma of hyperbolic heat conduction and its settlement by incorporating spatially nonlocal effect at nanoscale, *Phys. Lett. A* **380**, 255 (2016).
- [62] X. Zhou, K. K. Tamma, and C. V. D. R. Anderson, On a new C- and F-processes heat conduction constitutive model and the associated generalized theory of dynamic thermoelasticity, *J. Therm. Stresses* **24**, 531 (2001).
- [63] K. K. Tamma and X. Zhou, Macroscale and microscale thermal transport and thermo-mechanical interactions: Some noteworthy perspectives, *J. Therm. Stresses* **21**, 405 (1998).
- [64] H. B. Dwight, *Tables of Integrals and Other Mathematical Data* (Prentice Hall, Englewood Cliffs, NJ, 1961).